Title : will be set by the publisher
Editors : will be set by the publisher
EAS Publications Series, Vol. ?, 2002

FROM VISIBILITIES TO SCIENCE WITH SIMPLE MODELS

John Young[1]

Abstract. This is the manuscript of an "interactive seminar" from the programme of the EuroWinter School. These seminars were designed to illustrate areas of science that will be accessible to the VLTI and its first-generation instruments. This paper discusses the use of optical/IR interferometers to investigate the limb-darkening of stars, with particular emphasis on models with a one or two free parameters *i.e.* the kind of models that will be constrained by data from the first-generation VLTI. For this reason the paper is not a comprehensive treatment of limb-darkening measurement. Ideas from the introductory lectures of the School are illustrated here, using real data on a Mira variable star from the COAST interferometer.

1 Introduction

For several classes of stars, the angular resolution of approximately two milliarcseconds that will be achievable with the VLTI permits the study of features on finer scales than that of the stellar disk, including the limb-darkening profiles of the stars. However, we must ask why we are interested in making such measurements, and what is the best technique for securing them?

There are a number of reasons why it is important to measure limb-darkening. Accurate limb-darkening corrections must be made in order to measure precise effective temperatures. Knowledge of limb-darkening profiles is needed in order to interpret the light curves of eclipsing multiple systems, and also to fit models to interferometric data from a target in which other features (e.g. surface asymmetries or companion stars) are of interest. Finally, limb-darkening profiles provide an important diagnostic for stellar atmospheric models — one which has not been used extensively thus far.

As for measurement techniques, very few provide access to the high angular resolution needed for limb-darkening studies. Lunar occultations (e.g. Ridgway et al. 1982), gravitational microlensing (Albrow et al. 1999), and analysis of the light

[1] University of Cambridge, Astrophysics Group, Cavendish Laboratory, Madingley Road, Cambridge CB3 0HE, United Kingdom

DOI: (will be inserted later)

curves of eclipsing systems (Wilson and Devinney 1971) have all been used to some effect, but these can only be applied to certain targets at particular epochs. Hence there is a clear case for using interferometry for limb-darkening measurements.

This paper concentrates on the sub-topic of Mira variable limb-darkening, because real data has already been obtained using first-generation interferometers, and many Miras should be accessible to the VLTI, even in its early stages of development.

2 Fourier Space Representation of a Limb-Darkened Disk

Recall from Haniff (this volume) that, for a compact astronomical source, the complex visibility $V(u,v)$ is related to the sky brightness distribution $I(x,y)$ by a Fourier Transform:

$$V(u,v) = \int\int I(x,y) e^{-2\pi i(ux+vy)} dx\, dy. \tag{2.1}$$

In the case of a circularly-symmetric disk with centre-to-limb intensity profile $I(r)$ this reduces to the Hankel Transform

$$V(d_\lambda) = 2\pi \int I(r) J_0(d_\lambda r) r\, dr, \tag{2.2}$$

where d_λ is the projected length of the interferometer baseline in wavelengths.

An optical interferometer can usually measure the *amplitude* $|V|$ of the complex visibility, and possibly some quantity related to the phase of the visibility (closure phase, differential phase, ...). In the case of a circularly-symmetric disk $V(d_\lambda)$ is purely real (with sign changes), and the visibility amplitude is of most interest.

2.1 Limb-darkening parametrisations

I shall begin by discussing various empirical parametrisations of limb-darkening profiles. These are often used in the literature, and so anyone working in this field should be aware of them.

These so-called "limb-darkening laws" are useful in that they provide an approximation to a limb-darkening profile that can be described by a few parameters. If the number of parameters is small enough, one can hope to determine values for them from measurements with moderate angular resolution. Parametrisations are also useful when no detailed atmospheric model (which could otherwise be used to predict $I(r)$, and hence compared with the data) is available for a star of interest, or when the data disagree with all available models, as has happened in practice!

When working with empirical models, you should be aware that a given model will not necessarily be able to satisfactorily represent the true form of $I(r)$. If this is the case, then the values of the best-fit parameters (for example, the limb-darkened diameter) will have *no physical meaning*. There may also be more subtle problems that affect the model-fitting process.

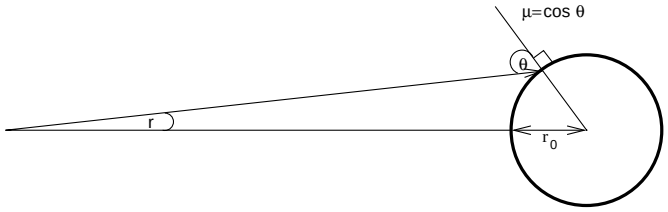

Fig. 1. Definition of the radial coordinate μ.

The empirical parametrisations that have been used in the literature are all expressed in terms of a reduced radial coordinate $\mu(r) = \sqrt{1 - \frac{r^2}{r_0^2}}$, where r is the angular radius of a particular point on the surface of the star *i.e.* μ is the cosine of the angle between the normal to the stellar surface at that point and the line of sight to the observer. The definition of μ is hopefully clarified by Fig. 1.

A comprehensive review of all parametrisations that have appeared in the literature was given by Burns (1997), who also derived their Hankel Transforms. Here two common parametrisations are presented as examples.

The parametrisation with the longest history is a straightforward Taylor expansion in μ, *i.e.*

$$\begin{aligned} \frac{I(r)}{I_0} &= 1 - \sum_{n=1}^{n_{\max}} \alpha_n \left(1 - \mu(r)\right)^n \quad r < r_0 \\ I(r) &= 0 \qquad\qquad\qquad\qquad\quad r > r_0 . \end{aligned} \tag{2.3}$$

The first- ($n_{\max} = 1$) and second-order ($n_{\max} = 2$) expansions are widely used to approximate the limb-darkening profiles of relatively hot stars.

A simpler parametrisation, due to Hestroffer (1997), can describe a wide range of limb-darkening, including extreme Gaussian-like profiles that approximate those of very cool stars in spectral bands contaminated by molecular absorption features:

$$\frac{I(r)}{I_0} = \mu^\alpha \quad r < r_0 . \tag{2.4}$$

Fig. 2 contrasts two very different parametrisations, a uniform disk (equivalent to a Hestroffer profile with $\alpha = 0$), and a Hestroffer profile with $\alpha = 1$. The intensity profiles, given by Eq. 2.4, are shown in the left-hand panel. The corresponding visibility curves at a wavelength of $1.3\,\mu$m, given by the Hankel Transform of Eq. 2.4 (Hestroffer 1997), are presented in the right-hand panel.

The angular diameter $2r_0$ of the Hestroffer model in Fig. 2 is 20 mas. The angular diameter of the uniform disk model has been chosen so that the visibility curves match at short baselines. The diameter needed to achieve this is 17.77 mas. The result that the visibility curves of a larger, more limb-darkened disk and a smaller, less limb-darkened disk can be almost identical on short baselines is

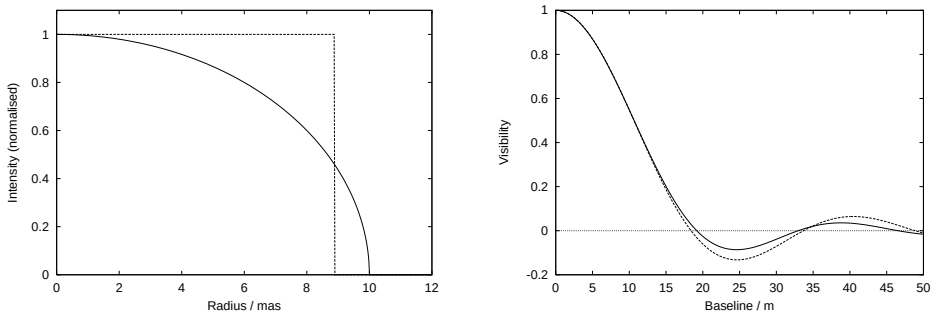

Fig. 2. Centre-to-limb intensity profiles (left-hand panel) and corresponding visibility curves (right-hand panel) for a uniform disk model (dashed lines) and a Hestroffer model with $\alpha = 1$ (solid lines). See text for more details.

true whatever limb-darkening parametrisations are chosen. This result has an important consequence if we want to measure the degree of limb-darkening: we must also measure the size of the stellar disk. This means measuring the visibility amplitude on at least two different baselines — this will be illustrated in Sec. 4.

3 Mira Limb-Darkening

I shall now discuss a particular type of limb-darkening measurement, the comparison of the observed limb-darkening profiles of Mira variables with the predictions of atmospheric models.

The particular atmospheric models discussed here are those of Hofmann et al. (1998) (henceforth HSW98). They incorporate both dynamical effects and realistic opacities. The models predict $I(\rho)$ (where ρ is a radial coordinate in metres) for a given observing bandpass, at a number of pulsation phases. Fundamental properties of the models discussed in this paper are summarized in Table 1 (note there are both fundamental-mode and first-overtone pulsators).

The models predict $I(\rho)$, which can be converted to $I(r)$ by specifying the angular diameter of the star, or equivalently, its distance. In contrast to the empirical parametrisations outlined in Sec. 2, there is only one free parameter, the angular diameter[1].

In the remainder of this paper, I shall consider a straightforward model-selection problem: which one of a small number of candidate Mira models is most probable, given a particular set of visibility data? The models each have one variable parameter, and so the most probable model will be the one with the smallest χ^2 (it is

[1] The dynamical models of HSW98 predict the variation in physical diameter with pulsation phase, so if you are fitting to measurements at multiple phases, you can choose to have just one free parameter for the entire set of measurements. Alternatively you can allow the diameter at each phase to be independent, ignoring the model-predicted variation.

Table 1. Fundamental properties of Mira models from HSW98. The E, P and M models labelled as "static" are the non-pulsating parent models from which the other, time-resolved models are derived.

Model	Pulsation Mode	Visual phase	$L/L_\odot$	$R/R_\odot$	$T_{\rm eff}$/K
E	static	–	6310	366	2700
E8300	1st overtone	0.83	4790	425	2330
E8380	1st overtone	1.00	6750	399	2620
E8560	1st overtone	1.21	7650	428	2610
P	static	–	3470	241	2860
P71800 = P05	fundamental	0.50	1650	289	2160
P73200 = P10	fundamental	1.00	5300	248	3130
M	static	–	3470	260	2750
M96400 = M05	fundamental	0.50	1470	242	2310
M97600 = M10	fundamental	1.00	4910	309	2750

more complicated to compare empirical models, which can have different numbers of parameters). The discussion of this specific topic will illustrate a number of general points concerning limb-darkening measurements.

3.1 Visibility Precision

Fig. 3 shows intensity profiles for the M10 fundamental-mode model and the E8380 overtone model (both are models of a Mira at maximum light). The angular diameters have been chosen so that the two models give identical visibility curves on short baselines. The observing passband is centred on 1.236 μm, and has a width of 0.012 μm. The differences between the profiles are much smaller than those in Fig. 2, and the differences in the visibility curves are correspondingly smaller. Indeed, distinguishing between the two models with measurements on moderate (< 30m) baselines, would require measurement of a $\sim 2\%$ visibility with an uncertainty of 2% of its value. Such a measurement is certainly not a good way of determining the pulsation mode of a Mira!

3.2 Angular Resolution

In order to distinguish the two models in Fig. 3 with measurements at a wavelength of 1.2 μm, a baseline of at least 25 m is needed. This corresponds to a resolution λ/d of 10 mas, compared with the stellar diameter of $\sim$22 mas.

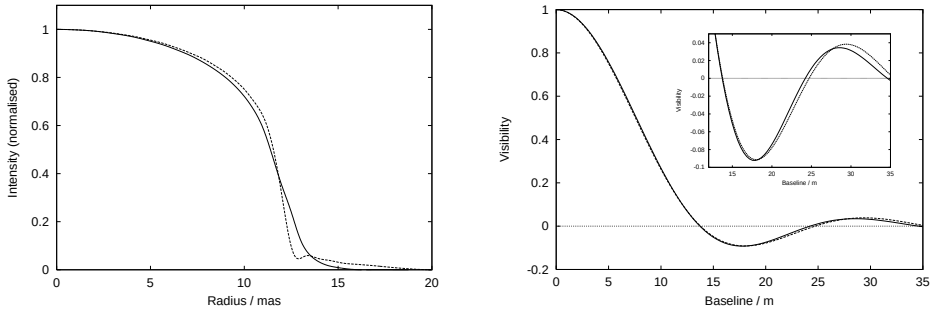

Fig. 3. 1.2 μm centre-to-limb intensity profiles (left-hand panel) and corresponding visibility curves (right-hand panel) for the M10 model from HSW98 (solid lines) and the E8380 model from the same paper (dashed lines). The inset in the right-hand panel shows part of the visibility plot in more detail.

3.3 Spectral Resolution

There are a number of constraints on the spectral resolution that must be used for interferometric measurements — refer to C. Haniff's second lecture (this volume) for details. For limb-darkening measurements, a further constraint is that the results be physically meaningful, *i.e.* that the radiation detected in each spectral channel originates from a reasonably narrow range of heights in the stellar atmosphere. This facilitates comparison with atmospheric models, and permits a reasonable estimate of the "diameter" in each spectral channel.

This requirement is more stringent for Mira variables, which have very extended atmospheres, than for other classes of stars. The near-infrared part of a model Mira spectrum is shown in Fig. 4. A spectral resolution $\lambda/\Delta\lambda$ of about 30 is required to isolate continuum emission in the J band, which is a good match for the low-dispersion mode of AMBER.

3.4 Sensitivity

The signal-to-noise for fringe measurement is a strong function of the visibility amplitude, and so the limiting sensitivity for highly resolved targets is many magnitudes worse than that for a point source.

That said, Mira variables are particularly bright in the near-infrared ($J \sim 0$ for the nearest examples), so sensitivity should not be an issue for measurements with AMBER.

3.5 Multiple baselines

As illustrated in Sec. 4 below, measurements on *at least* two baselines are required. For variable stars such as Miras, any reconfiguration of the array that is needed must obviously be performed swiftly.

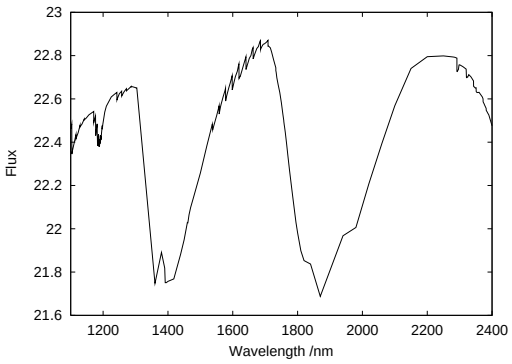

Fig. 4. Model Mira spectrum in the near-infrared region. Note the deep molecular absorption bands.

4 Example Data Analysis

In this section some of the points made above are illustrated by an example analysis of actual COAST data on the Mira χ Cygni. The observations were made on 18 July 1998, close to minimum light for χ Cyg. A single bandpass was used, centred on 1.29 μm with a width of 0.15 μm (*i.e.* somewhat wider than recommended in Sec. 3.3). As we shall see, the limb-darkening profiles for Miras near minimum light are more extreme than the maximum light profiles shown in Fig. 3, and less precise visibility measurements are needed to distinguish competing models.

Data were secured on all six baselines of the (then) four-element COAST array (Baldwin et al. 1994). Subsets of the data are presented, to find the minimum number of baselines that would have been needed to select the most appropriate intensity profile from those of the M05 and P05 models (see Table 1).

A visibility curve was computed from each model-predicted intensity profile, by calculating the Hankel Transform numerically, assuming a particular angular size. The value of χ^2 for any different model diameter could then be calculated by scaling the baselines of this visibility curve, making use of the Similarity Theorem of Fourier Transforms. A conjugate-gradient minimiser was employed to find the angular diameter that gave the minimum χ^2 value, given a particular initial guess at the diameter.

4.1 One Baseline

The analysis in this sub-section is obviously silly, but is included to reinforce the point made in Sec. 2 that measurements on at least two baselines are needed to determine angular size and limb-darkening independently.

As illustrated in Fig. 5, both the M05 and P05 models are good fits to the data on a single baseline (there is another solution for each model, not shown in

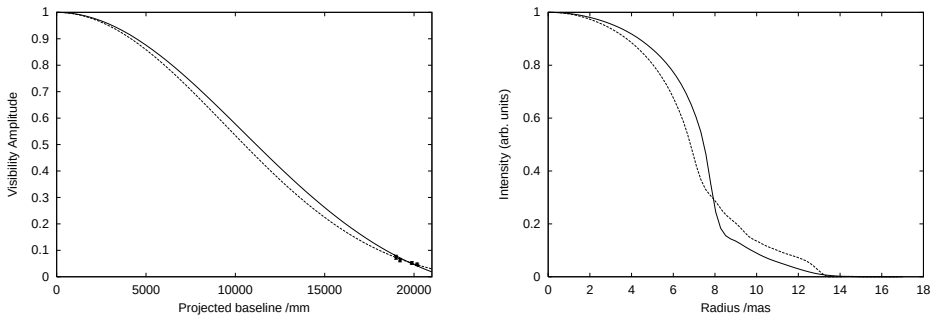

Fig. 5. Fits of intensity profiles from the M05 and P05 models of HSW98 to single-baseline COAST data. The data and visibility curves of the best-fitting M05 (solid line) and P05 (dashed line) models are plotted in the left-hand panel. The corresponding model intensity profiles are shown in the right-hand panel.

the figure, in which the measured points are past the first null in the visibility function).

The intensity profiles of the best-fit models, shown in the right-hand panel of Fig. 5, differ substantially. The profile of the P05 model has a more pronounced "wing" at large radius, making the profile almost Gaussian. The phrases "more limb-darkened" and "less limb-darkened" can scarcely be applied to such extreme shapes. Given a suitable definition of the "diameter" (see Baschek et al. 1991), it is possible to obtain the diameter values corresponding to the best-fit models.

4.2 Two Baselines

There are again two solutions for each of the M05 and P05 models. All four solutions are shown in Fig. 6. In the case of the M05 model, both solutions mis-fit the short baseline points, so we can reject this model as being incompatible with the data. One of the P05 solutions is a very poor fit (reduced $\chi^2 = 42$), whereas the other one (the solid line in the right-hand panel of Fig. 6) is acceptable (reduced $\chi^2 = 2.6$).

On the basis of this analysis we would prefer the P05 model, and can conclude that two baselines are sufficient to deduce this. We have been somewhat fortunate in our choice of baselines (because we could choose two from a set of six after the data were taken) — if we had to choose the baselines in advance for a star whose angular size was slightly uncertain, more baselines might have been needed.

The uv plane coverage for the data in Fig. 6 is shown in Fig. 7. The hour angle range of the data is 2 h 30 min, but the same number of data points (four on each of two baselines) could be secured in about 2 h with the VLTI, assuming that three Auxiliary Telescopes are present (and hence no moving of telescopes would be needed), and that the time taken to switch between measuring two different baselines is 15 min.

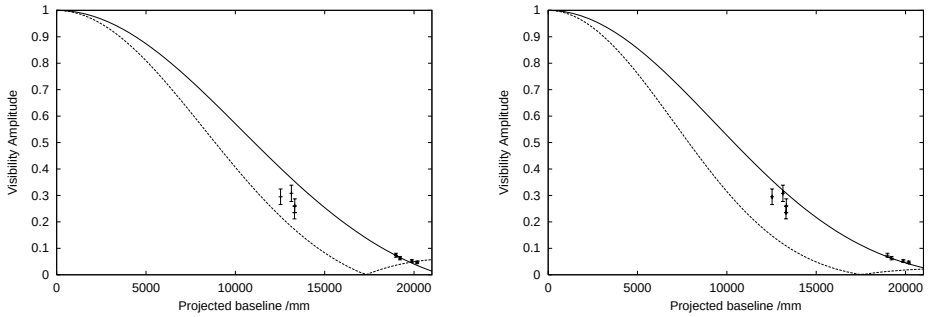

Fig. 6. Fits of intensity profiles from the M05 and P05 models of HSW98 to two-baseline COAST data. The left-hand panel shows the data and the visibility curves for the two M05 solutions, and the right-hand panel shows the two solutions for the P05 model. The intensity profiles themselves are not shown (they are simply scaled versions of the profiles in Fig. 5).

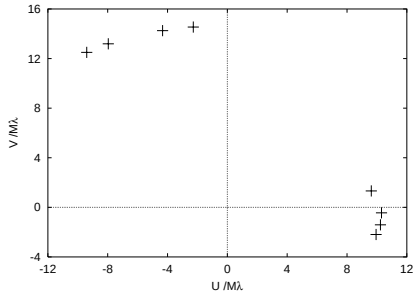

Fig. 7. uv plane coverage for the data presented in Fig. 6.

4.3 Six Baselines

The full dataset is shown in Fig. 8. It confirms our conclusion that the P05 model is a good fit (reduced $\chi^2 = 1.5$), and that the M05 model is inconsistent with the data. It is worth noting that a Gaussian intensity profile is a better fit to the data than the P05 model, which suggests that the remaining discrepancy between the P05 model and the data is real.

5 Conclusion

It is clear that limb-darkening measurements with the VLTI and its first-generation instruments are feasible for Mira variable stars. Such measurements should also be possible for other types of target, provided that the requirements of sufficient angular resolution and sensitivity are met.

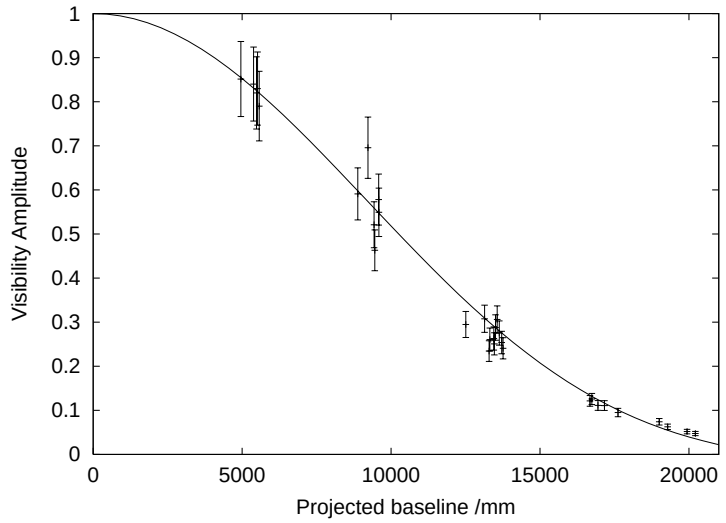

Fig. 8. Plot of the full COAST dataset, which includes data from six different baselines. The curve is the best-fitting P05 model.

References

Albrow, M. D., Beaulieu, J.-P., Caldwell, J. A. R., Dominik, M., Greenhill, J., Hill, K., Kane, S., Martin, R., Menzies, J., Naber, R. M., Pel, J.-W., Pollard, K., Sackett, P. D., Sahu, K. C., Vermaak, P., Watson, R., Williams, A., and Sahu, M. S.: 1999, *ApJ* **522**, 1011

Baldwin, J. E., Boysen, R. C., Cox, G. C., Haniff, C. A., Rogers, J., Warner, P. J., Wilson, D. M. A., and Mackay, C. D.: 1994, in J. B. Breckenridge (ed.), *Amplitude and Intensity Spatial Interferometry II*, Vol. 2200 of *Proc. SPIE*, pp 118–128, 15–16 Mar. 1994, Kona, Hawaii, SPIE

Baschek, B., Scholz, M., and Wehrse, R.: 1991, *A&A* **246**, 374

Burns, D.: 1997, *Ph.D. thesis*, Univ. Cambridge

Hestroffer, D.: 1997, *A&A* **327**, 199

Hofmann, K.-H., Scholz, M., and Wood, P. R.: 1998, *A&A* **339**, 846

Ridgway, S. T., Jacoby, G. H., Joyce, R. R., Siegel, M. J., and Wells, D. C.: 1982, *AJ* **87**, 1044

Wilson, R. E. and Devinney, E. J.: 1971, *ApJ* **166**, 605